

Amortized Simulation-Based Inference in Generalized Bayes via Neural Posterior Estimation

Shiyi Sun¹ Geoff K. Nicholls¹ Jeong Eun Lee²

Abstract

Generalized Bayesian Inference (GBI) tempers a loss with a temperature $\beta > 0$ to mitigate overconfidence and improve robustness under model misspecification, but existing GBI methods typically rely on costly MCMC or SDE-based samplers and must be re-run for each new dataset and each β -value. We give the first fully amortized variational approximation to the tempered posterior family $p_\beta(\theta | x) \propto \pi(\theta)p(x | \theta)^\beta$ by training a single (x, β) -conditioned neural posterior estimator $q_\phi(\theta | x, \beta)$ that enables sampling in a single forward pass, without simulator calls or inference-time MCMC. We introduce two complementary training routes: (i) synthesizes off-manifold samples $(\theta, x) \sim \pi(\theta)p(x | \theta)^\beta$ and (ii) reweights a fixed base dataset $\pi(\theta)p(x | \theta)$ using self-normalized importance sampling (SNIS), where we show that the SNIS-weighted objective provides a consistent forward-KL fit to the tempered posterior with finite weight variance. Across four standard simulation-based inference (SBI) benchmarks—including the chaotic Lorenz-96 system—our β -amortized estimator achieves competitive posterior approximations, in standard two-sample metrics, with non-amortized MCMC-based power-posterior samplers over a wide range of temperatures.

1. Introduction

Simulation-based inference (SBI) (Cranmer et al., 2020) addresses Bayesian inference when the likelihood is implicit, yet a simulator can generate samples. Given parameters θ , one can simulate $x \sim p(x | \theta)$ even though

¹Department of Statistics, University of Oxford, Oxford, United Kingdom ²Department of Statistics, University of Auckland, Auckland, New Zealand. Correspondence to: Shiyi Sun <shiyi.sun@spc.ox.ac.uk>.

Preprint. February 2, 2026.

the likelihood $p(x | \theta)$ is intractable (Lueckmann et al., 2021). This setting is common in scientific and engineering domains where complex mechanistic models can produce synthetic data, but evaluating or differentiating the likelihood is infeasible (Alsing et al., 2019; Lueckmann et al., 2017). Methods span from approximate Bayesian computation (ABC) (Beaumont et al., 2002; Marjoram et al., 2003) to neural posterior estimation (NPE) (Greenberg et al., 2019; Papamakarios & Murray, 2016) and neural likelihood/ratio estimation (NLE/NRE) (Papamakarios et al., 2019; Hermans et al., 2020; Durkan et al., 2020; Thomas et al., 2022). Many modern approaches further employ amortized inference (Greenberg et al., 2019; Papamakarios et al., 2019; Durkan et al., 2020; Gonçalves et al., 2020; Radev et al., 2020; Elsemüller et al., 2024), training neural networks that map simulated data directly to posterior or likelihood surrogates. Amortization enables efficient reuse across multiple observations and substantially lowers per-dataset inference cost compared with classical sampling-based methods (Lueckmann et al., 2021), but it typically presumes a well-specified simulator and that targeting the exact Bayesian posterior is desirable.

However, in practice, simulators are imperfect representations of reality: model misspecification and measurement noise can cause the Bayesian posterior to concentrate on pseudo-true regions that need not correspond to meaningful or stable solutions (Berk, 1966; Kleijn & van der Vaart, 2006; Grünwald & Van Ommen, 2017). To address such issues, generalized Bayesian inference (GBI) (Bissiri et al., 2016) updates beliefs using a loss-based surrogate in place of the likelihood. This approach can be rigorously justified through the lens of optimization-centric variational inference (Knoblauch et al., 2022), providing a principled route to robustness. Concretely, following (Bissiri et al., 2016), we write

$$L(\theta; x_{\text{obs}}) \equiv \exp\{-\beta l(\theta; x_{\text{obs}})\},$$

where $l(\theta; x_{\text{obs}})$ measures the quality of parameter θ relative to the observation and $\beta > 0$ is a temperature that balances data fit against the prior. With a prior $\pi(\theta)$ and simulator-defined likelihood $p(x | \theta)$, the

corresponding generalized posterior is

$$p(\theta | x_{\text{obs}}) \propto \exp\{-\beta l(\theta; x_{\text{obs}})\} \pi(\theta).$$

Choosing $l(\theta; x_{\text{obs}}) = -\log p(x_{\text{obs}} | \theta)$ yields the tempered (power) posterior (Friel & Pettitt, 2008; Marinari & Parisi, 1992), which preserves the likelihood-based structure while introducing a tunable robustness via β (down-weighting data for $\beta < 1$, up-weighting for $\beta > 1$). Related robustness perspectives include (Holmes & Walker, 2017; Lyddon et al., 2019), and practical choices of β can be calibrated to achieve nominal frequentist properties (Syring & Martin, 2019).

While generalized bayes provides a principled route to robustness, applying it to simulator-based settings remains challenging: evaluating the loss or scoring-rule expectations typically requires many simulator queries at inference time. Two recent strands address this gap. (i) Scoring-rule posteriors: Pacchiardi et al. (2024) replace the likelihood by strictly proper scoring rules (e.g., energy and kernel scores) to obtain a generalized posterior with consistency and outlier-robustness guarantees; inference is performed via pseudo-marginal MCMC or stochastic-gradient MCMC and is not amortized across observations. (ii) Amortized cost estimation (ACE): Gao et al. (2023) train a neural network to approximate the expected cost used in the GBI update, thereby amortizing cost evaluation and avoiding simulator calls at test time; samples from the generalized posterior are then obtained with MCMC over parameters. Both strands reduce reliance on explicit likelihoods but still require inference-time sampling over θ , which limits throughput when many x_{obs} must be processed or computational resources are constrained. This motivates our approach of directly amortizing the family of power posteriors $p_\beta(\theta | x)$ with NPE.

Contribution. Building on generalized Bayes, we focus on the power posterior

$$p_\beta(\theta | x) \propto \pi(\theta) p(x | \theta)^\beta, \quad (1)$$

which interpolates between the prior ($\beta \rightarrow 0$) and the standard posterior ($\beta = 1$). Whereas existing approaches typically require inference-time MCMC or SDE/score-based samplers to draw from $p_\beta(\theta | x)$, we propose a fully amortized alternative over both x and β that directly learns the family of power posteriors via neural posterior estimation (NPE). Concretely, we train a β -conditioned estimator $q_\phi(\theta | x, \beta)$ so that sampling from $p_\beta(\theta | x)$ at test time reduces to a single forward pass—without simulator calls or any MCMC.

We instantiate this idea through two complementary training routes:

- **Route A — Tempered-joint synthesis.** We build an offline dataset of (θ, x, β) by approximately sampling from the (unnormalized) tempered joint density, $p_\beta(\theta, x) \propto \pi(\theta) p(x | \theta)^\beta$. To approximate this joint, we learn the joint score $\nabla_{(\theta, x)} \log\{\pi(\theta) p(x | \theta)^\beta\}$ and use short-run Langevin dynamics across a temperature schedule to synthesize tempered pairs. Training NPE on these pairs lets the amortized model directly learn $p_\beta(\theta | x)$.
- **Route B — SNIS-weighted NPE (global per- β normalization).** Draw a base dataset $(\theta_i, x_i)_{i=1}^N \sim \pi(\theta) p(x | \theta)$ once and reuse it across temperatures. For any $m(x) > 0$, define the tempered joint $\pi_\beta(\theta, x) \propto \pi(\theta) p(x | \theta)^\beta m(x)$, whose conditional equals $p_\beta(\theta | x)$. Using the base joint as proposal, the self-normalized importance weight is

$$w_\beta(\theta, x) = \frac{\pi_\beta(\theta, x)}{\pi(\theta) p(x | \theta)} = p(x | \theta)^{\beta-1} m(x).$$

We fit a single amortized $q_\phi(\theta | x, \beta)$ by a per-temperature SNIS-weighted NPE objective.

We then minimize the objective

$$\mathcal{L}_{\text{SNIS}}(\phi) = - \sum_{\beta \in \mathcal{B}} \sum_{i=1}^N \tilde{w}_{\beta, i} \log q_\phi(\theta_i | x_i, \beta).$$

where $\tilde{w}_{\beta, i} \propto w_\beta(\theta_i, x_i)$. Two practical instantiations are: (i) NLE-based with $m(x) = 1$, plugging a learned $\hat{p}_\eta(x | \theta)$ for $p(x | \theta)$; (ii) NRE-based with $m(x) = p(x)^{1-\beta}$, where a classifier ratio $\hat{r}_\psi(x | \theta) \approx p(x | \theta) / p(x)$ yields $w_\beta(\theta, x) \propto \hat{r}_\psi(\theta, x)^{\beta-1}$.

Route B resembles Sequential Neural Variational Inference (SNVI) (Glöckler et al., 2022): SNVI makes a variational NPE-approximation to a posterior; the likelihood used to form the target-posterior is an NLE-approximation made using SBI. The NPE is not amortized. We target GBI and amortize data and β but similarly have an NPE objective targeting an NLE approximation.

2. Problem Setup

Following the fully amortized objective introduced above, we now formalize the learning problem. Let $\Theta \subseteq \mathbb{R}^{d_\theta}$ and $\mathcal{X} \subseteq \mathbb{R}^{d_x}$ be measurable spaces, $\pi(\theta)$ a prior, and $x \sim p(\cdot | \theta)$ an implicit simulator. For $\beta \in \mathcal{B}$, define the power posterior in (1) with normalizer $Z_\beta(x) = \int_\Theta \pi(\theta) p(x | \theta)^\beta d\theta < \infty$. Our goal is to learn a single amortized estimator $q_\phi(\theta | x, \beta)$ that approximates $p_\beta(\theta | x)$ for any β in a prescribed set \mathcal{B} (a discrete grid or a closed interval). At test time, β is

user-specified; during training, $\beta \sim p(\beta)$ supported on \mathcal{B} to ensure coverage.

Temperature constraints. As $\beta \downarrow 0$, $p_\beta(\theta | x) \rightarrow \pi(\theta)$; at $\beta = 1$ we recover standard Bayes; for $0 < \beta < 1$ the likelihood is down-weighted (typically improving robustness under misspecification), while $\beta > 1$ up-weights the likelihood and often yields tighter posteriors under well-specified simulators. To avoid degeneracy and guarantee $Z_\beta(x) < \infty$, we restrict β to a bounded domain $\mathcal{B} = [\beta_{\min}, \beta_{\max}]$ (or its grid) with $0 < \beta_{\min} \leq 1 \leq \beta_{\max} < \infty$, chosen for numerical stability.

3. Related work

Neural estimators for SBI. Modern SBI amortizes either the posterior, likelihood, or likelihood ratio from simulated pairs (Papamakarios & Murray, 2016; Greenberg et al., 2019; Papamakarios et al., 2019; Hermans et al., 2020; Durkan et al., 2020; Thomas et al., 2022). These approaches enable fast reuse across observations but typically target the standard Bayesian posterior ($\beta = 1$); recent studies examine calibration/robustness under misspecification (Cannon et al., 2022).

Generalized Bayes in SBI. Generalized Bayes replaces the likelihood by a loss-based update with a temperature β (Bissiri et al., 2016; Holmes & Walker, 2017; Lyddon et al., 2019). Within SBI, Gao et al. (2023) amortize the expected cost (ACE) and subsequently draw parameter samples via MCMC for each data set x_0 at test time. Algorithm 1 provides a brief summary of their procedure. Pacchiardi et al. (2024) instead construct scoring-rule posteriors using strictly proper scoring rules (e.g., energy or kernel scores) and perform pseudo-marginal or SG-MCMC inference, but their approach is not amortized at test time. Carmona & Nicholls (2022) and Battaglia & Nicholls (2024) amortize GBI *hyperparameters* using conditional normalizing flows and reverse-KL (rKL) variational inference, pointing to the difficulty of amortizing over data in GBI as a reason for relying on rKL minimization. In contrast, our work directly amortizes the family $p_\beta(\theta | x)$ across both observations x and the GBI hyperparameter β within the SBI framework, thereby avoiding both test-time MCMC and retraining.

Score-based synthesis. Score-based models learn the score $\nabla \log p$ via denoising score matching (Hyvärinen & Dayan, 2005; Vincent, 2011; Song & Ermon, 2019). A closely related alternative is to learn a conditional posterior score $s_\psi(\theta, t; x) \approx \nabla_\theta \log p_t(\theta | x)$ (equivalently, a conditional diffusion model in θ given (x, β)), so that score evaluation amortizes jointly over obser-

Algorithm 1 Gao et al. (2023): Generalized Bayes via ACE + MCMC

Inputs: prior $\pi(\theta)$, simulator $p(x | \theta)$, loss ℓ , temperature β .

- 1: Learn $C_\phi(\theta, x) \approx \mathbb{E}_{x' \sim p(\cdot | \theta)}[\ell(x', x)]$ (x -amortised surrogate) by regression on pairs (θ, x) (ACE).
- 2: Define $\log \tilde{p}_\beta(\theta | x_0) = \log \pi(\theta) - \beta C_\phi(\theta, x_0)$ (un-normalized).
- 3: Run MCMC targeting $\tilde{p}_\beta(\theta | x_0)$ to draw $\{\theta^{(s)}\}$.

vations and inverse temperatures. However, unlike a one-shot posterior sampler, generating samples at test time still requires running an iterative reverse-time procedure—e.g., predictor–corrector sampling or short-run Langevin dynamics—for each new observation x (and each β) (Geffner et al., 2023; Sharrock et al., 2022), which can dominate inference latency.

Route A (section 4.1) uses a learned joint score over (θ, x) purely as an offline generator (short-run Langevin across β) to create tempered training pairs, while inference uses a standard amortized posterior network. While we implement NCSN for concreteness, the route is agnostic to the scoring paradigm: VE/VP score-SDE frameworks (Song et al., 2020) and EDM (Karras et al., 2022) can be dropped in as alternatives (replacing the noise scale by a time parameter), with predictor–corrector or short-run Langevin samplers yielding the same NPE training objective.

IS-aware/forward-KL objectives. For a fixed temperature β , our objective

$$\mathcal{L}_\beta(\phi) = \mathbb{E}_{(\theta, x) \sim \pi_\beta}[-\log q_\phi(\theta | x, \beta)]$$

is a forward-KL (fKL) fit $\mathbb{E}_x \text{KL}(p_\beta(\theta | x) \| q_\phi(\theta | x, \beta))$ —a mass-covering criterion (Minka, 2005; Hernandez-Lobato et al., 2016; Li & Turner, 2016). Because $\pi_\beta(\theta, x) \propto \pi(\theta) p(x | \theta)^\beta m(x)$ can't be sampled directly, we estimate \mathcal{L}_β with self-normalized importance sampling (SNIS) (Murphy, 2012), using the joint $\pi(\theta)p(x | \theta)$ as proposal. The resulting weighted MLE, $\hat{\mathcal{L}}_\beta(\phi) = \sum_i \tilde{w}_{i,\beta} [-\log q_\phi(\theta_i | x_i, \beta)]$, has gradients that equal the SNIS estimate of the fKL gradient. This connects Route B to a long line of work on proposal learning by fKL and SNIS, including adaptive/mixture-boosting IS (Cappé et al., 2008; Cornuet et al., 2012; Jerfel et al., 2021) and the wake/sleep family where the inference network q is trained by $\text{KL}(p \| q)$ using (re)weighted samples (Hinton et al., 1995; Bornschein & Bengio, 2014). In our setting, the “proposal” being refined is the conditional $q_\phi(\theta | x, \beta)$ (e.g., a Mixture Density Network), giving an amortized fKL refinement across both x and β .

4. Amortized Power Posteriors via NPE

We amortize the family of power posteriors (1) by training a single β -conditioned NPE $q_\phi(\theta | x, \beta)$, enabling single-pass sampling for any (x, β) without simulator calls or inference-time MCMC. We realize this via two routes: (A) score-assisted synthesis of tempered triplets (θ, x, β) ; (B) reuse of a base joint dataset with per- β self-normalized importance weights (NLE/NRE instantiations). Implementation details and trade-offs follow.

4.1. Route A: score-assisted tempered synthesis + NPE

Algorithm 2 Route A: score-assisted tempered synthesis + NPE

Require: prior $\pi(\theta)$, simulator $p(x | \theta)$, noise scales $\{\sigma_t\}$, β -grid \mathcal{G} defining $p(\beta)$
Ensure: amortized posterior $q_\phi(\theta | x, \beta)$

- 1: **Phase I: learn joint score s_ψ (DSM).**
- 2: **for** minibatches $(\theta, x) \sim \pi(\theta)p(x | \theta)$ **do**
- 3: sample $\sigma \in \{\sigma_t\}$, $\epsilon \sim \mathcal{N}(0, I)$; set $(\tilde{\theta}, \tilde{x}) = (\theta, x) + \sigma\epsilon$
- 4: update ψ by minimizing $\|s_\psi(\tilde{\theta}, \tilde{x}, \sigma) + \epsilon/\sigma\|^2 \times \frac{1}{\sigma}$
- 5: **end for**
- 6: **Phase II: synthesize tempered pairs (short-run Langevin).**
- 7: **for** $\beta \sim p(\beta)$ **do**
- 8: initialize $(\theta_0, x_0) \sim \pi(\theta_0)p(x | \theta_0)$
- 9: **for** $t = 0, \dots, K-1$ **do**
- 10: $g_t \leftarrow \beta s_\psi(\theta_t, x_t, \sigma^*) - (\beta - 1)(s_\pi(\theta_t), 0)$
 with $s_\pi = \nabla_\theta \log \pi$
- 11: $(\theta_{t+1}, x_{t+1}) \leftarrow (\theta_t, x_t) + \eta_t g_t + \sqrt{2\eta_t} \xi_t$,
 $\xi_t \sim \mathcal{N}(0, I)$
- 12: **end for**
- 13: add (θ_K, x_K, β) to dataset \mathcal{D}
- 14: **end for**
- 15: **Phase III: Train NPE.**
- 16: Minimize $\min_\phi \mathbb{E}_{(\theta, x, \beta) \in \mathcal{D}} [-\log q_\phi(\theta | x, \beta)]$

A natural way to train a NPE targeting power posterior (1) is to construct a training set of (θ, x, β) triples which is distributed as the tempered joint

$$\tilde{p}_\beta(\theta, x) \propto \pi(\theta) p(x | \theta)^\beta \quad (2)$$

when conditioned on β . If $c_\beta(\theta) = \int p(x | \theta)^\beta dx$ then the marginal, $\tilde{p}_\beta(\theta) \propto \pi(\theta) c_\beta(\theta)$, is not the prior (except at $\beta = 1$) and $\tilde{p}_\beta(x | \theta) = p(x | \theta)^\beta / c_\beta(\theta)$ has unwanted θ and β dependence, but $c_\beta(\theta)$ cancels in the joint $\tilde{p}_\beta(\theta) \tilde{p}_\beta(x | \theta)$, so MCMC targeting (2) gives pairs (θ, x) with the property that $\theta | x \sim p_\beta(\theta | x)$ in (1).

We first learn a joint score $s_\psi(\theta, x) \approx \nabla_{(\theta, x)} \log p(\theta, x)$ using NCSN (Song & Ermon, 2019) on samples from the base joint distribution $p(\theta, x) = \pi(\theta)p(x | \theta)$. We then synthesize tempered pairs by running Langevin dy-

namics targeting tempered joint distribution $\tilde{p}_\beta(\theta, x)$:

$$(\theta^{k+1}, x^{k+1}) \leftarrow (\theta^k, x^k) + \eta \underbrace{\nabla_{(\theta, x)} \log \tilde{p}_\beta(\theta^k, x^k)}_{\text{use score} + \text{prior} + \beta} + \sqrt{2\eta} \xi^k. \quad (3)$$

with $\xi^k \sim \mathcal{N}(0, I)$ an annealed noise scheduled step size η . The joint score $s(\theta, x) = \nabla_{(\theta, x)} \log p(\theta, x)$ is

$$\begin{aligned} \nabla_{(\theta, x)} \log p(\theta, x) &= \nabla_{(\theta, x)} \log \pi(\theta) + \nabla_{(\theta, x)} \log p(x | \theta) \\ &= \left(\nabla_\theta \log \pi(\theta) \right) + \left(\nabla_x \log p(x | \theta) \right). \end{aligned} \quad (4)$$

To obtain $\nabla_{(\theta, x)} \log \tilde{p}_\beta(\theta, x)$, we can rewrite it in the following way:

$$\begin{aligned} \nabla_{(\theta, x)} \log \tilde{p}_\beta(\theta, x) &= \nabla_{(\theta, x)} \log \pi(\theta) + \beta \nabla_{(\theta, x)} \log p(x | \theta) \\ &= \beta \nabla_{(\theta, x)} \log p(\theta, x) \\ &\quad - (\beta - 1) (\nabla_\theta \log \pi(\theta), \mathbf{0}) \\ &\approx \beta s_\psi(\theta, x) - (\beta - 1) (\nabla_\theta \log \pi(\theta), \mathbf{0}). \end{aligned} \quad (5)$$

where in the first equality we substitute (2), in the second we note $\nabla_x \log \pi(\theta) = 0$ and apply Bayes' rule and finally $s_\psi(\theta, x) \approx s(\theta, x)$ from Algorithm 2.

Training objective. Once a large training set $\mathcal{D}_\beta = \{(\theta, x)\}$ is generated for multiple β values (sampled from some $p(\beta)$), we fit q_ϕ as a conditional MLE:

$$\min_\phi \mathbb{E}_{\beta \sim p(\beta)} \mathbb{E}_{(\theta, x) \sim \mathcal{D}_\beta} [-\log q_\phi(\theta | x, \beta)]. \quad (6)$$

The algorithm for Route A is given in Algorithm 2, more details about the selection of hyperparameters are in Appendix A.1.

4.2. Route B: Using SNIS to reweight the NPE (no scores, no MCMC)

On the joint space, consider the tempered family

$$\pi_\beta(\theta, x) \propto \pi(\theta) p(x | \theta)^\beta m(x), \quad m(x) > 0, \quad (7)$$

for which the conditional is unchanged for any $m(x)$: $\pi_\beta(\theta | x) = p_\beta(\theta | x) \propto \pi(\theta) p(x | \theta)^\beta$. Here $m(x)$ will be used to accommodate different likelihood estimators. To amortize $p_\beta(\theta | x)$ with a β -conditioned NPE $q_\phi(\theta | x, \beta)$, we would like to minimize

$$\mathcal{L}_\phi := \mathbb{E}_{(\theta, x) \sim \pi_\beta} [-\log q_\phi(\theta | x, \beta)]. \quad (8)$$

Sampling from $\pi_\beta(\theta, x)$ is not possible, so we use self-normalized importance sampling (SNIS) (Murphy,

2012) to reweight the base joint $p(\theta, x) = \pi(\theta)p(x | \theta)$. The unnormalized joint importance weight is

$$w_\beta(\theta, x) = \frac{\pi(\theta)p(x | \theta)^\beta m(x)}{\pi(\theta)p(x | \theta)} = p(x | \theta)^{\beta-1} m(x). \quad (9)$$

Two practical choices for $m(x)$.

- $m(x) = 1$ (**NLE-based**): $w_\beta(\theta, x) = p(x | \theta)^{\beta-1}$, approximated by $\hat{p}_\eta(x | \theta)$, a conditional likelihood trained using an NLE (Papamakarios et al., 2019).
- $m(x) = p(x)^{1-\beta}$ (**NRE-based**): the weights are $w_\beta(\theta, x) = \left(\frac{p(x|\theta)}{p(x)}\right)^{\beta-1}$, which can be acquired from a classifier-based likelihood-ratio estimator $\hat{r}_\psi(x | \theta)$ (NRE) via $\hat{r}_\psi = \frac{d_\psi}{1-d_\psi}$ with equal class priors (Hermans et al., 2020).

In both cases, we normalize the weights $\tilde{w}_\beta(\theta, x) = \frac{w_\beta(\theta, x)}{\sum w_\beta(\theta, x)}$. By the self-normalized importance sampling identity (Murphy, 2012), the objective is

$$\mathcal{L}_\phi = \frac{\mathbb{E}_{(\theta, x) \sim p(x, \theta)}[w_\beta(\theta, x)(-\log q_\phi(\theta | x, \beta))]}{\mathbb{E}_{(\theta, x) \sim p(x, \theta)}[w_\beta(\theta, x)]}. \quad (10)$$

We estimate (10) with

$$\begin{aligned} \hat{\mathcal{L}}_\phi(\beta) &= \frac{\sum_{i=1}^N w_{\beta, i} (-\log q_\phi(\theta_i | x_i, \beta))}{\sum_{i=1}^N w_{\beta, i}} \\ &= \sum_{i=1}^N \tilde{w}_{\beta, i} (-\log q_\phi(\theta_i | x_i, \beta)), \end{aligned} \quad (11)$$

where $\tilde{w}_{\beta, i} := \frac{w_{\beta, i}}{\sum_{j=1}^N w_{\beta, j}}$.

Minimizing (10) is equivalent to minimizing the fKL from the tempered posterior to q_ϕ , formalized below.

Proposition 4.1. *For any $\beta \in \mathcal{B}$,*

$$\arg \min_{\phi} \mathcal{L}_\phi = \arg \min_{\phi} \mathbb{E}_x [\text{KL}(p_\beta(\theta | x) \| q_\phi(\theta | x, \beta))].$$

The full proof is given in Appendix B.

In importance sampling, the dispersion of the weights is critical. For the NRE-based construction, with weights defined in (9), we establish the following.

Proposition 4.2. *The variance of the NRE weights is finite for $\beta \in [1/2, 1]$:*

$$\text{Var}[w_\beta] < 1.$$

A complete statement and proof are provided in Appendix B.

Both choices (NLE-based and NRE-based) instantiate the same SNVI target $\pi_\beta(\theta | x)$. We implement both and compare their performance on different benchmarks. In Algorithm (3) we give the NRE-based SNIS. The algorithm for NLE-based SNIS is similar, just using replacing NRE with NLE. The architecture of the neural net is given in Appendix A.2

Algorithm 3 Route B: SNIS-weighted NPE (NRE-based)

Require: prior $\pi(\theta)$, simulator $p(x | \theta)$, β -grid \mathcal{G} , ratio net d_ψ , NPE q_ϕ
Ensure: amortized posterior $q_\phi(\theta | x, \beta)$

- Base data:** draw $(\theta_i, x_i) \sim \pi(\theta)p(x | \theta)$ and negatives $(\tilde{\theta}_i, \tilde{x}_i) \sim \pi(\theta)p(x)$ for $i = 1..N$
- Train ratio (NRE-B):** minimize $\mathcal{L}_\psi = \frac{1}{N} \sum_i [-\log d_\psi(\theta_i, x_i) - \log(1 - d_\psi(\tilde{\theta}_i, \tilde{x}_i))]$
- compute $s_i = \log \hat{r}_\psi(x_i | \theta_i)$ with $\hat{r}_\psi = \frac{d_\psi}{1 - d_\psi}$
- for** $\beta \in \mathcal{G}$ **do** {global log-normalizer per temperature}
- $S_\beta \leftarrow \log(\sum_{i=1..N} \exp((\beta - 1)s_i))$
- set $\tilde{w}_i = \exp((\beta_i - 1)s_i - S_{\beta_i})$ for $i = 1..N$
- end for**
- Train NPE (SNIS weights):**
- minimize $\mathcal{L}_\phi = \frac{N}{|\mathcal{B}|} \sum_{i \in \mathcal{B}} \tilde{w}_i [-\log q_\phi(\theta_i | x_i, \beta_i)]$ for each batch \mathcal{B} ¹

5. Experiments

5.1. Benchmark

We evaluate β -amortized posterior inference by comparing samples from a single β -conditioned estimator $q_\phi(\theta | x, \beta)$ to reference samples from the corresponding power posterior $p_\beta(\theta | x) \propto \pi(\theta)p(x | \theta)^\beta$.

Experiments are conducted on four standard SBI benchmarks (Lueckmann et al., 2021; Lorenz, 1996) (Gaussian Mixture, Two Moons, SLCP, and Lorenz-96), chosen to span increasing posterior complexity from low-dimensional multimodality to chaotic dynamics. We report sample-based two-sample discrepancies (MMD (Gretton et al., 2012) and C2ST (Friedman, 2004; Lopez-Paz & Oquab, 2016)) as functions of β , and study the effect of simulation budget (10k vs. 100k) to quantify both temperature-robustness and data-efficiency. We further compare Route A (score-assisted tempered-pair synthesis) and Route B (SNIS-weighted NPE reweighting) to evaluate approximation fidelity under different amortization budgets and design choices. Full benchmark definitions, reference samplers, hyperparameters, and evaluation details are provided in Appendix C and Appendix D.

¹The mini-batch gradient in Step 9 is an unbiased estimator of the full-data weighted objective. A complete proof is given in Appendix B.

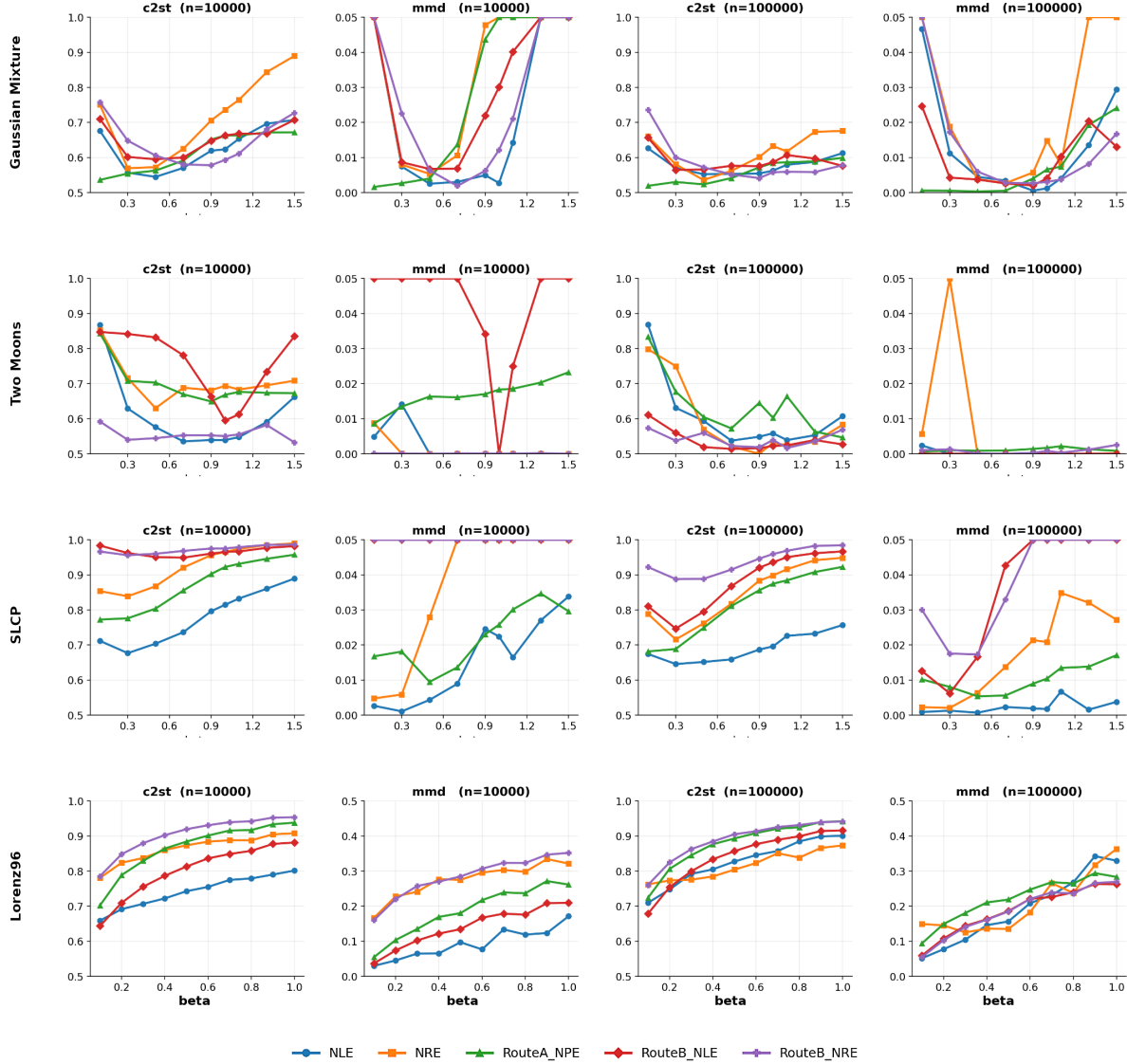


Figure 1. Route A/B comparison across benchmarks with a shared legend.

Figure 1 shows that our β -conditioned estimator $q_\phi(\theta | x, \beta)$ closely matches the ground-truth power posteriors $p_\beta(\theta | x)$ across benchmarks and temperatures, achieving low MMD and near-chance C2ST without inference-time MCMC. **Route B** (SNIS-weighted NPE) is typically the most efficient choice when β is not far from 1 (especially for $\beta \leq 1$), where reweighting is comparatively stable. **Route A** (score-assisted synthesis) is most useful when SNIS reweighting becomes unreliable (e.g., ratio/likelihood miscalibration or ESS collapse at small β) or when the base joint undercovers tempered regions; it can improve support coverage at the cost of additional offline compute and potential bias from score error and short-run Langevin dynamics. For additional intuition on how β reshapes the posterior

geometry, see Appendix F (Figs. 4–5).

Route-A does well at small β in the Gaussian mixture (dominating even non-amortised methods) and SLCP tests as the weight variance for Route-B SNIS methods climbs. At $\beta < 1$, SNIS-weighted NPE is approximating a diffuse target using a more concentrated importance sampling distribution so the red and purple curves trend up in C2ST and MMD losses at small β . All methods, amortized or not, show higher loss approximating the more structured posteriors at $\beta \rightarrow 1$. Route A generates training samples via short-run annealed Langevin dynamics and is exposed to miss-weighting strongly multimodal distributions (Two Moons). However, across all experiments the am-

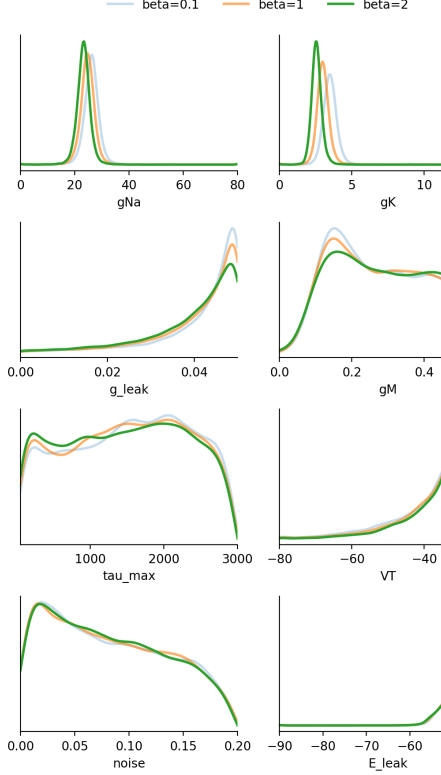


Figure 2. HH parameter marginals under `RouteB_NLE` for $\beta \in \{0.1, 1.0, 2.0\}$ (10K simulations).

tized methods are comparable with the non-amortised methods and sometimes out-perform them.

5.2. Single-Compartment Hodgkin–Huxley

We evaluate our method on a challenging scientific simulator, the single-compartment Hodgkin–Huxley (HH) model of neuronal voltage dynamics (Teeter et al., 2018; Pospischil et al., 2008). Following prior work (Gonçalves et al., 2020), the simulator has eight parameters and we use seven summary statistics computed from the voltage trace as observations. Full HH model details (parameter definitions, priors, and summary statistics) are provided in Appendix E. We perform inference for real electrophysiological recordings from the Allen Cell Types Database (Allen Institute for Brain Science, 2016), a setting known to be difficult due to model mismatch and experimental variability (Gao et al., 2023; Tolley et al., 2024).

We train our β -conditional posterior estimator using `RouteB-NLE` with 10,000 prior-sampled simulations. Figure 2 shows the one-dimensional marginal posteriors for the eight HH parameters under $\beta \in \{0.1, 1.0, 2.0\}$. The marginals are broadly consistent across β , with only modest shifts in a subset of parameters (visible

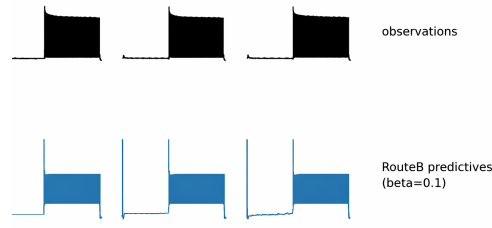


Figure 3. Three observations from the Allen Cell Types Database and `RouteB-NLE` predictive samples.

changes in the tails/peaks for g_{Na} and g_K while others remain nearly unchanged (E_{leak}). Figure 3 provides a posterior predictive check on three selected experimental sweeps: simulations generated from samples of $q_\phi(\theta | x_{obs}, \beta)$ at $\beta = 0.1$ qualitatively reproduce the observed spiking patterns, with predicted traces capturing the main spike timing structure across the three observations. Overall, these results indicate that `RouteB_NLE` trained with 10K simulations yields stable posterior marginals across β and produces posterior predictive simulations that match key qualitative features of the experimental voltage traces.

6. Route-specific trade-offs and limitations

As with all amortized inference schemes, our approach incurs substantial offline simulation and training cost. When simulation is prohibitively expensive or the data-generating process drifts after training, per-instance inference via adaptive sampling can be more cost-effective and robust (Gutmann & Corander, 2016). Our contribution should therefore be viewed as complementary to, rather than a replacement for, traditional adaptive inference.

Route A. Route A relies critically on the accuracy and stability of the learned joint score. Errors in the score estimator propagate through the annealing path and can be amplified at large inverse temperatures. Moreover, posterior sampling requires short-run Langevin or related MCMC procedures, whose performance is sensitive to discretization steps, noise schedules, and the number of iterations. These hyperparameters must be carefully tuned and may behave poorly in the presence of sharp, multimodal, or weakly connected posterior geometries, particularly as β increase. At the same time, Route A offers a key advantage: by explicitly simulating from tempered joint

distributions, it can generate samples that move off the nominal simulator manifold. This capability is especially valuable under model misspecification, where the true data-generating process deviates from the assumed simulator and reweighting-based approaches may fail to recover missing support.

Route B. Route B avoids explicit MCMC and is therefore significantly faster at deployment time. However, its accuracy hinges on the quality and variance of the importance weights $w_\beta \propto \hat{p}_\eta(x | \theta)^{\beta-1}$ (NLE-based) and $w_\beta \propto \hat{r}^{\beta-1}$ (NRE-based). Classifier miscalibration or noisy likelihood-ratio estimates can lead to high-variance weights and severe effective sample size (ESS) collapse, especially when $|\beta - 1|$ is large or $\beta \rightarrow 0$. In such regimes, posterior estimates become unstable despite nominal amortization. Furthermore, reweighting cannot recover posterior regions that are entirely absent from the base joint distribution. If the nominal simulator undercovers regions emphasized by the tempered posterior, Route B fails regardless of sample size. In contrast to Route A, it therefore offers limited robustness to severe model misspecification.

Generalization. Both routes require a single conditional model $q_\phi(\theta | x, \beta)$ to generalize jointly over observations and inverse temperatures. Performance can degrade for β values outside the trained range \mathcal{B} or for rare and distribution-shifted observations. Furthermore, NPE inherits sensitivity to neural architecture and training hyperparameters, and suboptimal choices can lead to underfitting, mode dropping, or miscalibration, necessitating careful tuning and diagnostic checks (Lueckmann et al., 2021; Hermans et al., 2020). In addition, for small β the posterior is prior-dominated and inherits sensitivity to prior misspecification, consistent with observations in generalized Bayesian updating (Bissiri et al., 2016; Lyddon et al., 2019).

7. Conclusion and future work

We gave x, β -amortized posterior inference for generalized Bayesian inference via power posteriors, learning a single conditional model $q_\phi(\theta | x, \beta)$ that supports single-pass sampling at deployment for user-chosen temperatures. We instantiated two complementary training routes: (A) score-assisted synthesis of tempered pairs with offline distillation, and (B) sampler-free SNIS reweighting that reuses a base joint dataset across β . Across standard SBI benchmarks, the resulting amortized family closely tracks non-amortized tempered targets over a broad temperature range, while eliminating simulator calls and inference-time MCMC at test time. The remaining challenges are (i) coverage/weight

stability as $|\beta - 1|$ grows and (ii) offline cost when simulators are expensive.

Future work. A promising direction is to make the approach adaptive rather than fixed: use ESS/weight-dispersion to automatically select between Route B (when weights are stable) and Route A (when coverage is insufficient). Second, develop more robust reweighting via defensive mixtures, calibrated ratio/likelihood estimators and sequential importance sampling (using $q_\phi(\theta | x, \beta)$ as a prior) to control heavy-tailed weights beyond the provable regime. Finally, extend evaluation to real-world amortization settings (many datasets, shifting conditions) and study principled temperature selection as a robustness knob under misspecification.

Impact Statement

This work enables amortized inference for generalized posteriors across tempering values β , reducing the cost of robustness and sensitivity analyses in simulation-based inference. By supporting fast posterior and predictive queries after training, it can improve accessibility and lower repeated sampling and compute overhead. Risks include misuse of amortized approximations without calibration, or misinterpreting tempered posteriors as fully Bayesian posteriors under misspecification, which may yield misleading uncertainty. We recommend reporting calibration and posterior-predictive diagnostics, monitoring importance-weight stability (e.g., ESS), and validating against higher-fidelity samplers on a small subset when feasible.

References

- Allen Institute for Brain Science. Allen cell types database, 2016. URL <http://celltypes.brain-map.org/>. Accessed 26-01-2026.
- Alsing, J., Charnock, T., Feeney, S., and Wandelt, B. Fast likelihood-free cosmology with neural density estimators and active learning. *Monthly Notices of the Royal Astronomical Society*, 488(3):4440–4458, 2019.
- Ba, J. L., Kiros, J. R., and Hinton, G. E. Layer normalization. *arXiv preprint arXiv:1607.06450*, 2016.
- Battaglia, L. and Nicholls, G. Amortising variational bayesian inference over prior hyperparameters with a normalising flow. *arXiv preprint arXiv:2412.16419*, 2024.
- Beaumont, M. A., Zhang, W., and Balding, D. J. Approximate bayesian computation in population genetics. *Genetics*, 162(4):2025–2035, 2002.

Beaumont, M. A., Cornuet, J.-M., Marin, J.-M., and Robert, C. P. Adaptive approximate bayesian computation. *Biometrika*, 96(4):983–990, 2009.

Berk, R. H. Limiting behavior of posterior distributions when the model is incorrect. *The Annals of Mathematical Statistics*, 37(1):51–58, 1966.

Bishop, C. M. Mixture density networks. Technical Report NCRG/94/004, Aston University, Neural Computing Research Group, 1994.

Bissiri, P. G., Holmes, C. C., and Walker, S. G. A general framework for updating belief distributions. *Journal of the Royal Statistical Society Series B: Statistical Methodology*, 78(5):1103–1130, 2016.

Bornschein, J. and Bengio, Y. Reweighted wake-sleep. *arXiv preprint arXiv:1406.2751*, 2014.

Cannon, P., Ward, D., and Schmon, S. M. Investigating the impact of model misspecification in neural simulation-based inference. *arXiv preprint arXiv:2209.01845*, 2022.

Cappé, O., Douc, R., Guillin, A., Marin, J.-M., and Robert, C. P. Adaptive importance sampling in general mixture classes. *Statistics and Computing*, 18(4):447–459, 2008.

Carmona, C. U. and Nicholls, G. K. Scalable Semi-Modular Inference with Variational Meta-Posteriors, April 2022. URL <https://github.com/chriscarmona/modularbayes>. arXiv: 2204.00296.

Cornuet, J.-M., Marin, J.-M., Mira, A., and Robert, C. P. Adaptive multiple importance sampling. *Scandinavian Journal of Statistics*, 39(4):798–812, 2012.

Cranmer, K., Brehmer, J., and Louppe, G. The frontier of simulation-based inference. *Proceedings of the National Academy of Sciences*, 117(48):30055–30062, 2020.

Durkan, C., Murray, I., and Papamakarios, G. On contrastive learning for likelihood-free inference. In *International conference on machine learning*, pp. 2771–2781. PMLR, 2020.

Elsemüller, L., Olschläger, H., Schmitt, M., Bürkner, P.-C., Koethe, U., and Radev, S. T. Sensitivity-aware amortized bayesian inference. *Transactions on Machine Learning Research*, 2024. ISSN 2835-8856. URL <https://openreview.net/forum?id=Kxtpa9rvM0>.

Friedman, J. On multivariate goodness-of-fit and two-sample testing. Technical report, SLAC National Accelerator Laboratory (SLAC), Menlo Park, CA (United States), 2004.

Friel, N. and Pettitt, A. N. Marginal likelihood estimation via power posteriors. *Journal of the Royal Statistical Society Series B: Statistical Methodology*, 70(3):589–607, 2008.

Gao, R., Deistler, M., and Macke, J. H. Generalized bayesian inference for scientific simulators via amortized cost estimation. *Advances in Neural Information Processing Systems*, 36:80191–80219, 2023.

Geffner, T., Papamakarios, G., and Mnih, A. Compositional score modeling for simulation-based inference. In *International Conference on Machine Learning*, pp. 11098–11116. PMLR, 2023.

Glöckler, M., Deistler, M., and Macke, J. H. Variational methods for simulation-based inference. In *International Conference on Learning Representations*, 2022. URL <https://openreview.net/forum?id=kZOUYdhqkNY>.

Gonçalves, P. J., Lueckmann, J.-M., Deistler, M., Nonnenmacher, M., Öcal, K., Bassetto, G., Chintaluri, C., Podlaski, W. F., Haddad, S. A., Vogels, T. P., et al. Training deep neural density estimators to identify mechanistic models of neural dynamics. *elife*, 9: e56261, 2020.

Greenberg, D., Nonnenmacher, M., and Macke, J. Automatic posterior transformation for likelihood-free inference. In *International conference on machine learning*, pp. 2404–2414. PMLR, 2019.

Gretton, A., Borgwardt, K. M., Rasch, M. J., Schölkopf, B., and Smola, A. A kernel two-sample test. *The journal of machine learning research*, 13(1):723–773, 2012.

Grünwald, P. D. and Van Ommen, T. Inconsistency of Bayesian inference for Misspecified Linear Models, and a Proposal for Repairing It. *Bayesian Analysis*, 12(4):1069–1103, 2017. doi: 10.1214/17-BA1085.

Gutmann, M. U. and Corander, J. Bayesian optimization for likelihood-free inference of simulator-based statistical models. *Journal of Machine Learning Research*, 17(125):1–47, 2016.

He, K., Zhang, X., Ren, S., and Sun, J. Deep residual learning for image recognition. In *Proceedings of the IEEE conference on computer vision and pattern recognition*, pp. 770–778, 2016.

Hermans, J., Begy, V., and Louppe, G. Likelihood-free mcmc with amortized approximate ratio estimators.

In *International conference on machine learning*, pp. 4239–4248. PMLR, 2020.

Hernandez-Lobato, J., Li, Y., Rowland, M., Bui, T., Hernández-Lobato, D., and Turner, R. Black-box alpha divergence minimization. In *International conference on machine learning*, pp. 1511–1520. PMLR, 2016.

Hinton, G. E., Dayan, P., Frey, B. J., and Neal, R. M. The "wake-sleep" algorithm for unsupervised neural networks. *Science*, 268(5214):1158–1161, 1995.

Ho, J., Jain, A., and Abbeel, P. Denoising diffusion probabilistic models. *Advances in neural information processing systems*, 33:6840–6851, 2020.

Holmes, C. C. and Walker, S. G. Assigning a value to a power likelihood in a general bayesian model. *Biometrika*, 104(2):497–503, 2017.

Hyvärinen, A. and Dayan, P. Estimation of non-normalized statistical models by score matching. *Journal of Machine Learning Research*, 6(4), 2005.

Jerfel, G., Wang, S., Wong-Fannjiang, C., Heller, K. A., Ma, Y., and Jordan, M. I. Variational refinement for importance sampling using the forward kullback-leibler divergence. In *Uncertainty in Artificial Intelligence*, pp. 1819–1829. PMLR, 2021.

Karras, T., Aittala, M., Aila, T., and Laine, S. Elucidating the design space of diffusion-based generative models. *Advances in neural information processing systems*, 35:26565–26577, 2022.

Kleijn, B. and van der Vaart, A. Misspecification in infinite-dimensional bayesian statistics. *The Annals of Statistics*, 34(2):837–877, 2006. doi: 10.1214/00905360600000029. URL <https://doi.org/10.1214/00905360600000029>.

Knoblauch, J., Jewson, J., and Damoulas, T. An optimization-centric view on bayes' rule: Reviewing and generalizing variational inference. *Journal of Machine Learning Research*, 23(132):1–109, 2022.

Li, Y. and Turner, R. E. Rényi divergence variational inference. *Advances in neural information processing systems*, 29, 2016.

Lopez-Paz, D. and Oquab, M. Revisiting classifier two-sample tests. *arXiv preprint arXiv:1610.06545*, 2016.

Lorenz, E. N. Predictability: A problem partly solved. In *Proc. Seminar on predictability*, volume 1, pp. 1–18. Reading, 1996.

Lueckmann, J.-M., Goncalves, P. J., Bassetto, G., Öcal, K., Nonnenmacher, M., and Macke, J. H. Flexible statistical inference for mechanistic models of neural dynamics. *Advances in neural information processing systems*, 30, 2017.

Lueckmann, J.-M., Boelts, J., Greenberg, D., Goncalves, P., and Macke, J. Benchmarking simulation-based inference. In *International conference on artificial intelligence and statistics*, pp. 343–351. PMLR, 2021.

Lyddon, S. P., Holmes, C. C., and Walker, S. G. General bayesian updating and the loss-likelihood bootstrap. *Biometrika*, 106(2):465–478, 2019.

Marinari, E. and Parisi, G. Simulated tempering: a new monte carlo scheme. *Europhysics letters*, 19(6):451, 1992.

Marjoram, P., Molitor, J., Plagnol, V., and Tavaré, S. Markov chain monte carlo without likelihoods. *Proceedings of the National Academy of Sciences*, 100(26):15324–15328, 2003.

Minka, T. Divergence measures and message passing. Technical report, Microsoft Research, Tech. Rep. MSR-TR-2005-173, 2005.

Murphy, K. P. *Machine learning: a probabilistic perspective*. MIT press, 2012.

Nichol, A. Q. and Dhariwal, P. Improved denoising diffusion probabilistic models. In *International conference on machine learning*, pp. 8162–8171. PMLR, 2021.

Pacchiardi, L., Khoo, S., and Dutta, R. Generalized bayesian likelihood-free inference. *Electronic Journal of Statistics*, 18(2):3628–3686, 2024.

Papamakarios, G. and Murray, I. Fast ε -free inference of simulation models with bayesian conditional density estimation. *Advances in neural information processing systems*, 29, 2016.

Papamakarios, G., Sterratt, D., and Murray, I. Sequential neural likelihood: Fast likelihood-free inference with autoregressive flows. In *The 22nd international conference on artificial intelligence and statistics*, pp. 837–848. PMLR, 2019.

Papamakarios, G., Nalisnick, E., Rezende, D. J., Mohamed, S., and Lakshminarayanan, B. Normalizing flows for probabilistic modeling and inference. *Journal of Machine Learning Research*, 22(57):1–64, 2021.

Pospischil, M., Toledo-Rodriguez, M., Monier, C., Piwkowska, Z., Bal, T., Frégnac, Y., Markram, H., and Destexhe, A. Minimal Hodgkin-Huxley type models for different classes of cortical and thalamic neurons. *Biological cybernetics*, 99(4):427–441, 2008.

Radev, S. T., Mertens, U. K., Voss, A., Ardizzone, L., and Köthe, U. Bayesflow: Learning complex stochastic models with invertible neural networks. *IEEE transactions on neural networks and learning systems*, 33(4):1452–1466, 2020.

Sharrock, L., Simons, J., Liu, S., and Beaumont, M. Sequential neural score estimation: Likelihood-free inference with conditional score based diffusion models. *arXiv preprint arXiv:2210.04872*, 2022.

Simola, U., Cisewski-Kehe, J., Gutmann, M. U., and Corander, J. Adaptive approximate bayesian computation tolerance selection. *Bayesian analysis*, 16(2):397–423, 2021.

Sisson, S. A., Fan, Y., and Tanaka, M. M. Sequential monte carlo without likelihoods. *Proceedings of the National Academy of Sciences*, 104(6):1760–1765, 2007.

Song, Y. and Ermon, S. Generative modeling by estimating gradients of the data distribution. *Advances in neural information processing systems*, 32, 2019.

Song, Y., Sohl-Dickstein, J., Kingma, D. P., Kumar, A., Ermon, S., and Poole, B. Score-based generative modeling through stochastic differential equations. *arXiv preprint arXiv:2011.13456*, 2020.

Syring, N. and Martin, R. Calibrating general posterior credible regions. *Biometrika*, 106(2):479–486, 2019.

Teeter, C., Iyer, R., Menon, V., Gouwens, N., Feng, D., Berg, J., Szafer, A., Cain, N., Zeng, H., Hawrylycz, M., et al. Generalized leaky integrate-and-fire models classify multiple neuron types. *Nature communications*, 9(1):709, 2018.

Thomas, O., Dutta, R., Corander, J., Kaski, S., and Gutmann, M. U. Likelihood-free inference by ratio estimation. *Bayesian Analysis*, 17(1):1–31, 2022.

Tolley, N., Rodrigues, P. L., Gramfort, A., and Jones, S. R. Methods and considerations for estimating parameters in biophysically detailed neural models with simulation based inference. *PLOS Computational Biology*, 20(2):e1011108, 2024.

Toni, T., Welch, D., Strelkowa, N., Ipsen, A., and Stumpf, M. P. Approximate bayesian computation scheme for parameter inference and model selection in dynamical systems. *Journal of the Royal Society Interface*, 6(31):187–202, 2009.

Vincent, P. A connection between score matching and denoising autoencoders. *Neural computation*, 23(7):1661–1674, 2011.

Appendix

A. Neural architectures

All methods that use score modeling follow Noise Conditional Score Networks (NCSN) (Song & Ermon, 2019) on noisy pairs and Langevin-type sampling for tempered joints (Vincent, 2011; Hyvärinen & Dayan, 2005; Song & Ermon, 2019).

A.1. Score-assisted route(Route A)

The implementation details of the three phases of Algorithm 2 follow.

Phase I : Score network $s_\psi(\theta, x, \sigma)$ Concatenate $[e_\theta, e_x, e_\sigma]$ and map through a residual MLP to produce a joint score.

- Parameter embedding e_θ - Input is θ . MLP (width 128) with 3 residual blocks and LayerNorm after each block.
- Data embedding e_x - Input is x . MLP (width 128) with 3 residual blocks and LayerNorm after each block.
- Noise-scale embedding e_σ - Input is $\log \sigma$. 2-layer MLP (width 128) similar to time/noise embeddings used in diffusion models (Ho et al., 2020; Nichol & Dhariwal, 2021).

Phase II : Synthesize tempered pairs Geometric schedule $\{\gamma_t\}_{t=1}^T$ with $T=10$, $\gamma_{\min}=0.01$, $\gamma_{\max}=1.0$ (increasing). We use $\sigma_t = \sqrt{\gamma_t}$.

Phase III : Posterior estimator For each temperature, we train an SNPE posterior $q_\phi(\theta | x, \beta)$ using `sbi` with `density_estimator='nsf'` or `'mdn'` (Greenberg et al., 2019; Bishop, 1994). Settings: batch 128, `stop_after_epochs=50`, validation fraction 0.1.]

Architectural notes. All MLPs use residual connections (He et al., 2016) and LayerNorm (Ba et al., 2016). The design mirrors diffusion/score-modeling practice for conditioning on noise variables (Ho et al., 2020; Nichol & Dhariwal, 2021).

A.2. SNIS-weighted route (Route B)

- (i) *NLE*: learn a neural likelihood $\hat{p}_\eta(x | \theta)$ (Papamakarios et al., 2019); choose $m(x) = 1$ so the SNIS weight is $w_\beta(\theta, x) \propto \hat{p}_\eta(x | \theta)^{\beta-1}$.
- (ii) *NRE*: learn a classifier $d_\psi(\theta, x)$ that discriminates joint vs. product-of-marginals (Hermans et al., 2020; Durkan et al., 2020; Thomas et al., 2022); set $\hat{r}_\psi = \frac{d_\psi}{1-d_\psi}$ and use $m(x) = p(x)^{1-\beta}$, giving $w_\beta(\theta, x) \propto \hat{r}_\psi(x | \theta)^{\beta-1}$.

Inference. For an observation x_{obs} and temperature β , form the context $[z(x_{\text{obs}}), \beta]$ (with z an identity or learned summary) and draw samples from $q_\phi(\theta | x_{\text{obs}}, \beta)$ in a single forward pass—no simulator or MCMC.

Notes. MDNs work well for low-dimensional multi-modal posteriors; in higher dimensions use flow-based q_ϕ (e.g., MAF/NSF) or other conditional estimators (Papamakarios et al., 2021).

B. Proof of proposition

Setup. Let $\Theta \subseteq \mathbb{R}^{d_\theta}$ and $\mathcal{X} \subseteq \mathbb{R}^{d_x}$ be measurable spaces. Define the base joint distribution with density $p(\theta, x) = \pi(\theta)p(x | \theta)$. For $\beta > 0$, the tempered joint (unnormalized) is defined as $\tilde{p}_\beta(\theta, x) = \pi(\theta)p(x | \theta)^\beta m(x)$, where $m(x) > 0$ for any $x \in \mathcal{X}$. And its x-marginal $\tilde{p}_\beta(x) = \int \pi(\theta)p(x | \theta)^\beta d\theta m(x)$

Therefore, the conditional distribution can be written as

$$p_\beta(\theta | x) = \frac{\tilde{p}_\beta(\theta, x)}{\tilde{p}_\beta(x)} = \frac{\pi(\theta)p(x | \theta)^\beta}{\int \pi(\theta)p(x | \theta)^\beta d\theta} \propto \pi(\theta)p(x | \theta)^\beta. \quad (12)$$

which is usually the definition of the power posterior

$$p_\beta(\theta | x) = \frac{\pi(\theta)p(x | \theta)^\beta}{\tilde{p}_\beta(x)}. \quad (13)$$

Define the weights as:

$$w_\beta(\theta, x) = p(x | \theta)^{\beta-1}m(x), m(x) > 0 \quad (14)$$

We train $q_\phi(\theta | x, \beta)$ by weighted conditional MLE on samples from $p(x, \theta)$:

$$\mathcal{L}(\phi) = \mathbb{E}_{(\theta, x) \sim p(\theta, x)} [\tilde{w}_\beta(\theta, x) \cdot (-\log q_\phi(\theta | x, \beta))], \quad \tilde{w}_\beta(\theta, x) \propto w_\beta(\theta, x). \quad (15)$$

Lemma B.1. *For any measurable $g : \Theta \times \mathcal{X} \rightarrow \mathbb{R}$,*

$$\int g(\theta, x) p(\theta, x) p(x | \theta)^{\beta-1} m(x) d\theta dx = \int g(\theta, x) \tilde{p}_\beta(\theta, x) d\theta dx \quad (16)$$

$$= \int \left(\int g(\theta, x) p_\beta(\theta | x) d\theta \right) \tilde{p}_\beta(x) dx. \quad (17)$$

Proof.

$$\int g(\theta, x) p(\theta, x) p(x | \theta)^{\beta-1} m(x) d\theta dx = \int g(\theta, x) \pi(\theta) p(x | \theta)^\beta m(x) d\theta dx \quad (18)$$

$$= \int g(\theta, x) \tilde{p}_\beta(\theta, x) d\theta dx \quad (19)$$

where we used the decomposition of the base joint distribution and the definition of the tempered joint distribution, which proves (16). For (17), write $\tilde{p}_\beta(\theta, x) = p_\beta(\theta | x) \tilde{p}_\beta(x)$ and apply Fubini/Tonelli to exchange the order of integration:

$$\int g(\theta, x) \tilde{p}_\beta(\theta, x) d\theta dx = \int \left(\int g(\theta, x) p_\beta(\theta | x) d\theta \right) \tilde{p}_\beta(x) dx$$

□

Proposition 4.1: Assume $\rho_\beta(x) > 0$ for p_β -almost all x and that the model class for $q_\phi(\cdot | x, \beta)$ contains $p_\beta(\cdot | x)$. Then the population minimizers of (15) satisfy, for p_β -almost all x ,

$$\arg \min_{\phi} \mathcal{L}(\phi) = \arg \min_{\phi} \int \rho_\beta(x) \text{KL}(p_\beta(\cdot | x) \| q_\phi(\cdot | x, \beta)) dx. \quad (20)$$

Proof. By Lemma 1, up to a positive constant the objective equals

$$\mathcal{L}(\phi) \propto \int \left[\int (-\log q_\phi(\theta | x, \beta)) p_\beta(\theta | x) d\theta \right] \tilde{p}_\beta(x) dx \quad (21)$$

$$= \int \left(H(p_\beta(\cdot | x)) + \text{KL}(p_\beta(\cdot | x) \| q_\phi(\cdot | x, \beta)) \right) \tilde{p}_\beta(x) dx \quad (22)$$

$$= \int H(p_\beta(\cdot | x)) \tilde{p}_\beta(x) dx + \int \text{KL}(p_\beta(\cdot | x) \| q_\phi(\cdot | x, \beta)) \tilde{p}_\beta(x) dx. \quad (23)$$

Here $H(\cdot)$ is the conditional entropy, independent of ϕ . Since $\rho_\beta(x) > 0$, the integral is minimized iff $\text{KL}(p_\beta(\cdot | x) \| q_\phi(\cdot | x, \beta)) = 0$ for p_β -a.e. x . This happens exactly when $q_\phi(\cdot | x, \beta) = p_\beta(\cdot | x)$ almost everywhere.

Then we have

$$\arg \min_{\phi} \mathcal{L}(\phi) = \arg \min_{\phi} \int \rho_{\beta}(x) \text{KL}(p_{\beta}(\cdot | x) \| q_{\phi}(\cdot | x, \beta)) dx. \quad (24)$$

□

Proposition 4.2. For $\beta \in [\frac{1}{2}, 1]$, with the NRE self-normalized IS weight

$$w_{\beta}(\theta, x) = p(x | \theta)^{\beta-1} p(x)^{1-\beta}.$$

Then

$$\mathbb{E}_{(\theta, x) \sim \pi(\theta)p(x|\theta)}[w_{\beta}^2] = \int_{\Theta} \int_{\mathcal{X}} \pi(\theta) p(x | \theta)^{2\beta-1} p(x)^{2-2\beta} dx d\theta \leq 1.$$

In particular, the SNIS estimator based on joint distribution $p(\theta, x)$ and w_{β} has finite variance.

Proof. Fix $\beta \in [\frac{1}{2}, 1]$. For $\beta = \frac{1}{2}$ we have

$$\int_{\mathcal{X}} p(x | \theta)^0 p(x)^1 dx = \int_{\mathcal{X}} p(x) dx = 1,$$

hence $\mathbb{E}_{p(\theta, x)}[w_{\frac{1}{2}}^2] = 1$.

For $\frac{1}{2} < \beta < 1$, set

$$u = \frac{1}{2\beta-1}, \quad v = \frac{1}{2-2\beta}, \quad \frac{1}{u} + \frac{1}{v} = 1, \quad u, v > 1.$$

By Hölder's inequality,

$$\int_{\mathcal{X}} p(x | \theta)^{2\beta-1} p(x)^{2-2\beta} dx = \int_{\mathcal{X}} (p(x | \theta))^{1/u} (p(x))^{1/v} dx \leq \left(\int p(x | \theta) dx \right)^{1/u} \left(\int p(x) dx \right)^{1/v} = 1.$$

Integrating the above bound against $\pi(\theta) d\theta$ yields $\mathbb{E}_{p(\theta, x)}[w_{\beta}^2] \leq 1$. Finite variance follows since $\text{Var}[w_{\beta}] = \mathbb{E}_{p(\theta, x)}[w_{\beta}^2] - E_{p(\theta, x)}[w_{\beta}]^2 < E_{p(\theta, x)}[w_{\beta}^2] < \infty$. □

Proposition B.2. Let $\{\ell_i(\phi)\}_{i=1}^N$ be differentiable per-sample losses with

$$\ell_i(\phi) = -\log q_{\phi}(\theta_i | x_i, \beta_i),$$

Fix the globally and locally normalized SNIS weights

$$\tilde{w}_{\beta, i}^G = \frac{w_{\beta, i}}{\sum_{j=1}^N w_{\beta, j}}, \quad \tilde{w}_{\beta, i}^L = \frac{w_{\beta, i}}{\sum_{j \in \mathcal{B}} w_{\beta, j}}.$$

Let $\mathcal{B} \subset \{1, \dots, N\}$ be a mini-batch of size $|\mathcal{B}| = b$. Define the global and local estimators

$$\hat{\mathcal{L}}_{\mathcal{B}}^G(\phi) = \frac{N}{b} \sum_{i \in \mathcal{B}} \tilde{w}_{\beta, i}^G \ell_i(\phi), \quad \hat{\mathcal{L}}_{\mathcal{B}}^L(\phi) = \frac{N}{b} \sum_{i \in \mathcal{B}} \tilde{w}_{\beta, i}^L \ell_i(\phi)$$

Then

$$\mathbb{E}_{\mathcal{B}}[\hat{\mathcal{L}}_{\mathcal{B}}^G(\phi)] = \sum_{i=1}^N \tilde{w}_{\beta, i}^G \ell_i(\phi), \quad \mathbb{E}_{\mathcal{B}}[\hat{\mathcal{L}}_{\mathcal{B}}^L(\phi)] \neq \sum_{i=1}^N \tilde{w}_{\beta, i}^G \ell_i(\phi)$$

Proof. For each i , let $\mathbf{1}\{i \in \mathcal{B}\}$ be the inclusion indicator. If \mathcal{B} is a uniform size- b subset (with or without replacement), then $\mathbb{P}(i \in \mathcal{B}) = b/N$. By linearity of expectation and of the gradient operator,

$$\mathbb{E}_{\mathcal{B}}[\widehat{\mathcal{L}}_{\mathcal{B}}(\phi)] = \frac{N}{b} \sum_{i=1}^N \tilde{w}_{\beta,i}^G \mathbb{E}_{\mathcal{B}}[\mathbf{1}\{i \in \mathcal{B}\}] \ell_i(\phi) = \sum_{i=1}^N \tilde{w}_{\beta,i}^G \ell_i(\phi).$$

In contrast,

$$\mathbb{E}_{\mathcal{B}}[\widehat{\mathcal{L}}_{\mathcal{B}}^{(L)}(\phi)] = \sum_{i=1}^N \alpha_i \ell_i(\phi), \quad \text{with } \alpha_i := \frac{N}{b} \mathbb{E}_{\mathcal{B}}\left[\frac{w_{\beta,i} \mathbf{1}\{i \in \mathcal{B}\}}{\sum_{j \in \mathcal{B}} w_{\beta,j}}\right].$$

To be unbiased for all losses $\{\ell_i\}$, we would need $\alpha_i = \tilde{w}_{\beta,i}^G$ for every i . However, this fails in general. A simple counterexample is $b = 1$: then $\sum_{j \in \mathcal{B}} w_{\beta,j} = w_{\beta,I}$ for the unique index $I \in \{1, \dots, N\}$, and

$$\alpha_i = N \mathbb{E}_{\mathcal{B}}\left[\frac{w_{\beta,i} \mathbf{1}\{i = I\}}{w_{\beta,I}}\right] = N \frac{1}{N} \cdot 1 = 1,$$

so

$$\mathbb{E}_{\mathcal{B}}[\widehat{\mathcal{L}}_{\mathcal{B}}^{(L)}(\phi)] = \sum_{i=1}^N \ell_i(\phi),$$

whereas $\widehat{\mathcal{L}}_{\phi}(\beta) = \sum_{i=1}^N \tilde{w}_{\beta,i}^G \ell_i(\phi)$ with $\sum_i \tilde{w}_{\beta,i}^G = 1$ and $\tilde{w}_{\beta,i}^G \neq 1$ unless all $w_{\beta,i}$ are equal. Hence, the locally normalized estimator is biased whenever the weights are non-constant. \square

C. Benchmark simulators and settings

C.1. Two Moons

Prior	$\mathcal{U}(-1, 1)$
Simulator	$x \mid \theta = \begin{bmatrix} r \cos \alpha + 0.25 \\ r \sin \alpha \end{bmatrix} + \begin{bmatrix} - \theta_1 + \theta_2 /\sqrt{2} \\ (-\theta_1 + \theta_2)/\sqrt{2} \end{bmatrix}, \alpha \sim \mathcal{U}(-\frac{\pi}{2}, \frac{\pi}{2}), r \sim \mathcal{N}(0.1, 0.01^2)$
Dimensionality	$\theta \in \mathbb{R}^2, x \in \mathbb{R}^2$
References	(Greenberg et al., 2019; Lueckmann et al., 2021)

C.2. Gaussian Mixture

Prior	$\mathcal{U}(-1, 1)$
Simulator	$x \mid \theta \sim \frac{1}{2} \mathcal{N}(\theta, I_2) + \frac{1}{2} \mathcal{N}(\theta, 0.01 I_2)$
Dimensionality	$\theta \in \mathbb{R}^2, x \in \mathbb{R}^2$
References	(Lueckmann et al., 2021; Sisson et al., 2007; Beaumont et al., 2009; Toni et al., 2009; Simola et al., 2021)

C.3. SLCP

Prior	$\mathcal{U}(-3, 3)$
Simulator	$x \mid \theta = (x_1, \dots, x_4), x_i \sim \mathcal{N}(\mathbf{m}_{\theta}, \mathbf{S}_{\theta}),$ $\mathbf{m}_{\theta} = \begin{bmatrix} \theta_1 \\ \theta_2 \end{bmatrix}, \mathbf{S}_{\theta} = \begin{bmatrix} s_1^2 & \rho s_1 s_2 \\ \rho s_1 s_2 & s_2^2 \end{bmatrix}, s_1 = \theta_3^2, s_2 = \theta_4^2, \rho = \tanh \theta_5.$
Dimensionality	$\theta \in \mathbb{R}^5, x \in \mathbb{R}^8$
References	(Lueckmann et al., 2021; Papamakarios et al., 2019; Greenberg et al., 2019; Hermans et al., 2020; Durkan et al., 2020)

C.4. Lorenz–96

Prior	$b_0 \sim \mathcal{U}[1.4, 2.2]$, $b_1 \sim \mathcal{U}[0.1, 1.0]$, $\sigma_e \sim \mathcal{U}[1.5, 2.5]$
Simulator	$x \mid \theta = (x_0, \dots, x_T)$, $x_t \in \mathbb{R}^K$, obtained by integrating

$$\frac{dx_k}{dt} = -x_{k-1}(x_{k-2} - x_{k+1}) - x_k + 10 - (b_0 + b_1 x_k + \sigma_e \eta_k(t)), \quad \eta_k(t) \sim \mathcal{N}(0, 1),$$

for $k = 1, \dots, K$, with cyclic indices.

Dimensionality $\theta \in \mathbb{R}^3$, $x \in \mathbb{R}^{(T+1) \times K}$

Fixed parameters State dimension $K = 8$; time step $\Delta t = 3/40$; trajectory length $T = 20$.
Initial condition $x_0 = \mathbf{1}_K$ (all ones).

References (Lorenz, 1996)

D. Ground-truth power posteriors.

For each benchmark and temperature $\beta \in \{0.1, 0.3, 0.5, 0.7, 0.9, 1.0, 1.1, 1.3, 1.5\}$, we generate high-quality samples from the power posterior $p_\beta(\theta \mid x) \propto \pi(\theta) p(x \mid \theta)^\beta$ as follows.

Two Moons. We use a tempered random-walk Metropolis–Hastings kernel inside the uniform prior box. Proposals are reflected at the box boundaries, and we apply a small support-projection step to ensure the simulator’s valid sector (implemented via the condition $v_x > 0$ in our likelihood). During burn-in we adapt the per-chain step sizes with a Robbins–Monro schedule to target an acceptance rate of 0.3. We run two chains initialized on opposite sides of the fold, burn in for 10,000 iterations, thin by 2, and then keep 5,000 states per chain, yielding 10,000 power posterior draws for each β . All computations use double precision.

Gaussian Mixture. We employ an independent rejection sampler that is exact for any $\beta > 0$. The proposal is a β -scaled Gaussian-mixture envelope $\sum_{i=1}^2 \tilde{w}_i(\beta) \mathcal{N}(\theta; x, \Sigma_i/\beta)$ with $\Sigma_1 = I$ and $\Sigma_2 = 0.01 I$, and weights $\tilde{w}_i(\beta) \propto (0.5)^{\max(\beta, 1)} K_\beta(\Sigma_i)$ (constant factors cancel in the acceptance ratio). A candidate outside the prior box is rejected; otherwise it is accepted with probability proportional to $[0.5 \mathcal{N}(\theta; x, I) + 0.5 \mathcal{N}(\theta; x, 0.01 I)]^\beta / G_\beta(\theta)$, where G_β denotes the envelope density. This yields 10,000 i.i.d. draws per temperature.

SLCP. We use a parallel-tempering random-walk Metropolis–Hastings sampler on the 5-dimensional box prior $\theta \sim \mathcal{U}([-3, 3]^5)$. For each target temperature β we construct a geometric ladder of $R = 200$ inverse temperatures between $\beta_{\min} = 0.01$ and β , ordered from hot to cold. Each replica runs a Gaussian random-walk within the prior box; proposals outside the box are rejected. The per-coordinate proposal scale at temperature β_r is set to $0.2/\sqrt{\beta_r}$ and is further adapted during burn-in via a Robbins–Monro schedule to target an average acceptance rate of 0.25. Between swap attempts, each chain performs 5 local MH updates, and every two iterations we attempt swaps between neighboring temperatures using an even–odd scheme. The temperature ladder is initialized by drawing 2048 prior samples and selecting the R highest-likelihood points as starting states. We run 15 000 iterations in total, discard the first 5 000 as burn-in, and then retain every cold-chain state, yielding 10 000 draws from the power posterior $p_\beta(\theta \mid x)$ for each β .

Lorenz–96. For the Lorenz–96 task we run a single-chain random-walk Metropolis–Hastings sampler on the 3-dimensional box prior $b_0 \sim \mathcal{U}[1.4, 2.2]$, $b_1 \sim \mathcal{U}[0.1, 1.0]$, $\sigma_e \sim \mathcal{U}[1.5, 2.5]$. Likelihoods are evaluated via precomputed sufficient statistics of the discretized Gaussian transition model, so that each evaluation is $\mathcal{O}(1)$ in the number of particles. For each β we initialize the chain by drawing 1500 prior samples, computing their likelihoods, and starting from the maximum-likelihood point. Proposals are Gaussian random-walks with independent components scaled to one sixth of the corresponding prior width; they are reflected at the box boundaries to enforce the prior support. During a tuning phase of 6 000 iterations we adapt a single global step factor using a Robbins–Monro scheme to target an acceptance rate of 0.3, with the acceptance probability based on the power posterior $p_\beta(\theta \mid x) \propto \pi(\theta) p(x \mid \theta)^\beta$ (the uniform prior cancels within the box). After tuning, we fix the step size and run 10 000 further MH iterations, collecting all states as reference draws from the power posterior for the given β .

E. Hodgkin–Huxley model

We follow the single-compartment Hodgkin–Huxley (HH) model used in prior SBI work (Gonçalves et al., 2020; Pospischil et al., 2008). The model describes the membrane potential dynamics of a neuron under a fixed current injection protocol via standard conductance-based equations with voltage-dependent gating variables.

Parameters. The simulator involves eight unknown parameters, $\theta = (g_{\text{Na}}, g_{\text{K}}, g_{\text{M}}, g_{\text{leak}}, -V_T, -E_{\text{leak}}, t_{\text{max}}, \sigma) \in \mathbb{R}^8$, where g_{Na} , g_{K} , g_{M} , and g_{leak} are maximal conductances for sodium, delayed-rectifier potassium, slow voltage-dependent potassium (M-type), and leak channels, respectively; $-V_T$ denotes an effective spiking threshold parameter; $-E_{\text{leak}}$ is the leak reversal potential; t_{max} controls the time scale of the stimulus (or the recording window) in the benchmark implementation; and σ denotes the observation noise level. (All parameter bounds and priors are taken from the benchmark specification.)

Observations and summary statistics. Given θ , the simulator produces a membrane-voltage trace $v(t)$, which we map to a 7-dimensional vector of summary statistics $x \in \mathbb{R}^7$. Specifically, we use the spike count, the mean resting potential, the standard deviation of the resting potential, and the first four central moments of the voltage trace (mean, standard deviation, skewness, and kurtosis), following (Gonçalves et al., 2020). These summary statistics constitute the observation used by all inference methods in the HH experiments.

F. Additional visualizations: effect of β on the posterior

To build intuition for how the power posterior changes with the tempering parameter β , we visualize samples from (i) a reference sampler and (ii) our two amortized routes on two toy problems (Gaussian mixture and two moons). In all panels, rows correspond to different β values, and columns compare the reference power posterior with Route A and Route B. As β decreases, the posterior becomes flatter and closer to the prior; as β increases, it concentrates around data-fitting regions.

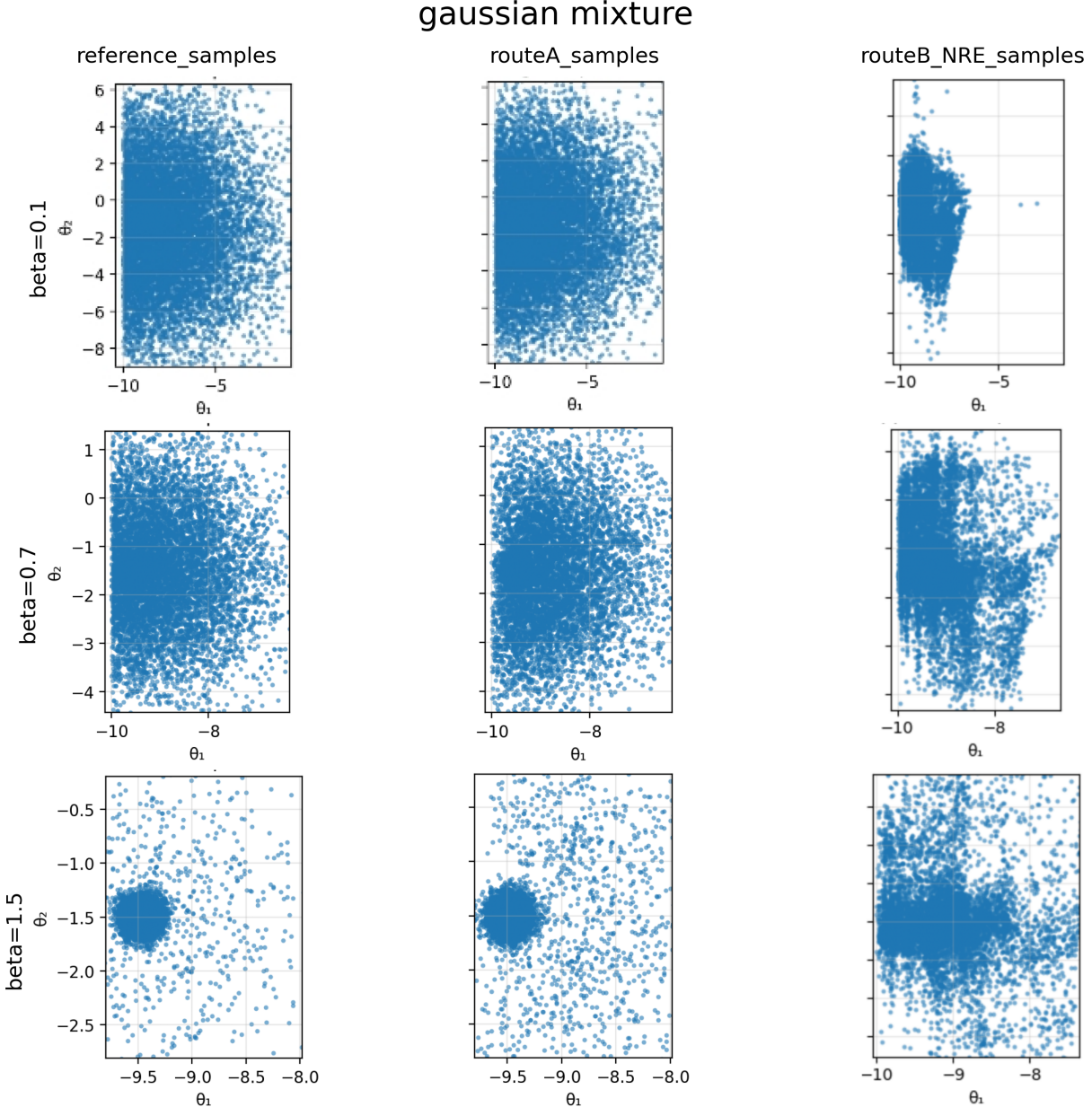


Figure 4. Gaussian mixture. Qualitative effect of the power posterior across different β values. Rows correspond to $\beta \in \{0.1, 0.7, 1.5\}$ and columns show samples from the reference power posterior (left), Route A (middle), and Route B (NRE-SNIS; right).

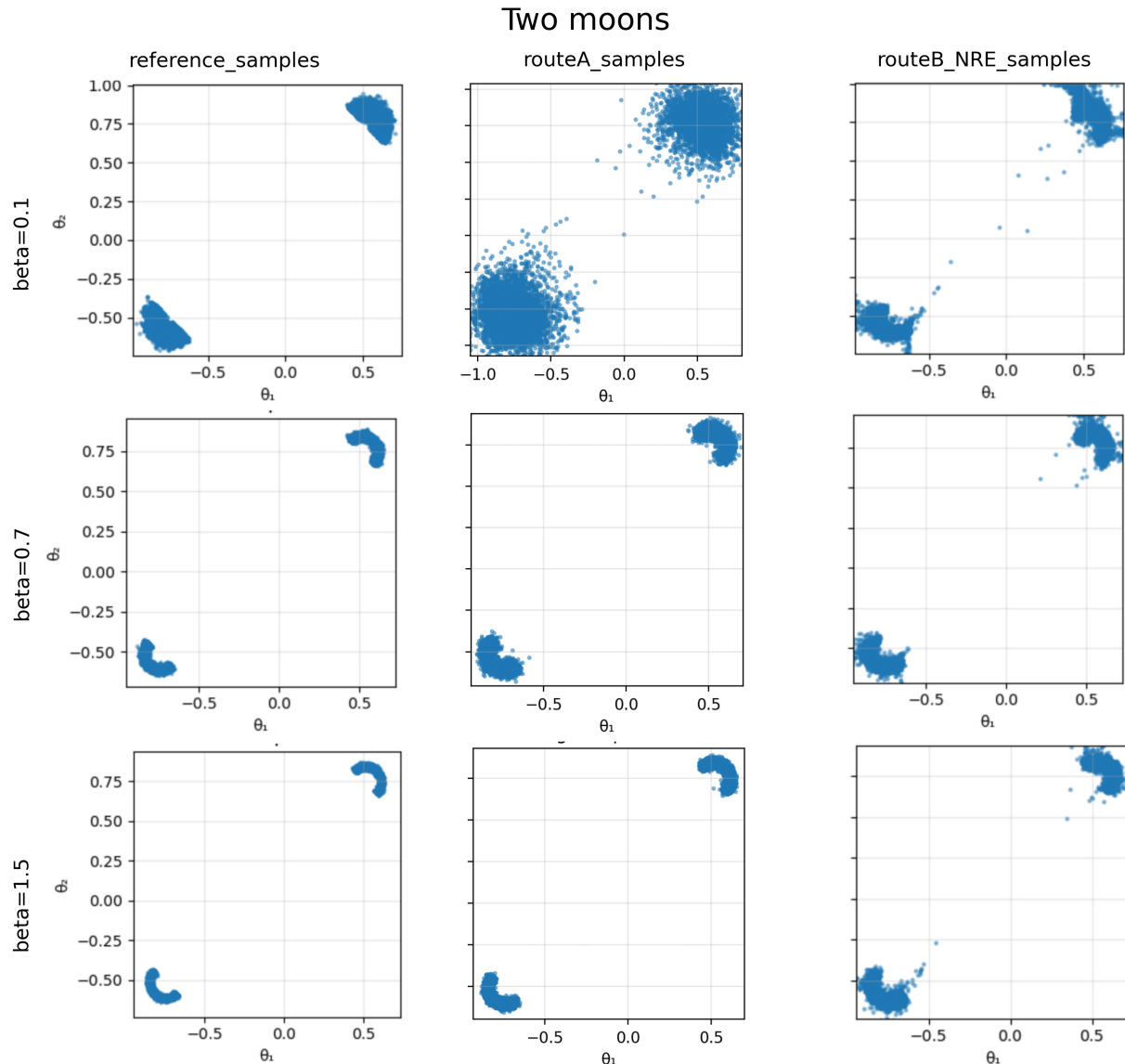


Figure 5. Two moons. Qualitative effect of the power posterior across different β values. Rows correspond to $\beta \in \{0.1, 0.7, 1.5\}$ and columns show samples from the reference power posterior (left), Route A (middle), and Route B (NRE-SNIS; right).